Lawrence Berkeley National Laboratory
Recent Work

Title
MICROSTRUCTURE OF LEAD TITANATE CERAMICS MODIFIED BY ALKALINE EARTH ELEMENTS

Permalink
https://escholarship.org/uc/item/1rk9m3g6

Author
Yamamoto, T.

Publication Date
1986-02-01

eScholarship.org Powered by the California Digital Library
University of California

LBL-21000
c.2

Lawrence Berkeley Laboratory
UNIVERSITY OF CALIFORNIA

RECEIVED
LAWRENCE
BERKELEY LABORATORY
AUG 12 1986
LIBRARY AND
DOCUMENTS SECTION

Materials & Molecular Research Division

MICROSTRUCTURE OF LEAD TITANATE CERAMICS MODIFIED BY ALKALINE EARTH ELEMENTS

T. Yamamoto, K. Okazaki, E. Goo, and G. Thomas

February 1986

TWO-WEEK LOAN COPY
This is a Library Circulating Copy which may be borrowed for two weeks.

Prepared for the U.S. Department of Energy under Contract DE-AC03-76SF00098

LBL-21000
c.2

DISCLAIMER

This document was prepared as an account of work sponsored by the United States Government. While this document is believed to contain correct information, neither the United States Government nor any agency thereof, nor the Regents of the University of California, nor any of their employees, makes any warranty, express or implied, or assumes any legal responsibility for the accuracy, completeness, or usefulness of any information, apparatus, product, or process disclosed, or represents that its use would not infringe privately owned rights. Reference herein to any specific commercial product, process, or service by its trade name, trademark, manufacturer, or otherwise, does not necessarily constitute or imply its endorsement, recommendation, or favoring by the United States Government or any agency thereof, or the Regents of the University of California. The views and opinions of authors expressed herein do not necessarily state or reflect those of the United States Government or any agency thereof or the Regents of the University of California.

Microstructure of Lead Titanate Ceramics modified by Alkaline Earth Elements

T. Yamamoto and K. Okazaki

National Defense Academy, Yokosuka, 239 Japan

and

E. Goo* and G. Thomas, Professor Materials Science and Mineral Engineering, University of California, Berkeley, CA 94720 and Scientific Director, National Center for Electron Microscopy, Materials and Molecular Research Division, Lawrence Berkeley Laboratory, Berkeley, CA 94720.

*Present Address: The Department of Materials Science, University of Southern California, University Park, Los Angeles, CA 90089.

Abstract

Microstructures in $(P_{b-x,}Me_x)_ATi_BO_3$ ceramics, (Me=Ca, Ba and Sr, x=0 to 0.4531, A/B=0.99) have been investigated. These alkaline earth element modified $PbTiO_3$ ceramics have typically large crystal anisotropy. Among these ceramics, the Ca and Ba modified ones exhibit unique microstructures compared to those of Sr modified $PbTiO_3$, viz., large crystal tetragonality, small grain size, multiple domain regions.

Introduction

Lead titanate, $PBTiO_3$ is well known as the end composition of the $PBTiO_3$-$PbZrO_3$ (PZT) system, which is widely used for electronic components. To date, almost all investigations of PZT have been conducted near the morphotropic phase boundary (MPB), $Pb(Zr_{0.53}Ti_{0.47})O_3$ because of the high piezoelectricity observed at this composition.

Shortly after the discovery of ferroelectricity in PZT ceramics, many efforts to obtain dense $PbTiO_3$ ceramics have been attempted. However, it was very difficult to fabricate high density $PbTiO_3$ ceramics, because pure $PbTiO_3$ ceramics breaks up into a powder when cooled through the Curie point (phase transition temperature). [1] Two methods to prepare dense $PbTiO_3$ ceramics can be classified as follows: one, by adding suitable additives [2] and the other is by combining with other compounds to form solid solutions.[3,4,5,6] By using these methods, unique properties of $PbTiO_3$ were gradually revealed. The Curie point is 490^o C, which is considerably higher than that of PZT. On the other hand, the relative permittivity at room temperature (RT) is about 1/3 to 1/10 smaller than that of PZT

ceramics. In addition, a markedly large anisotropy in piezoelectric coupling factor has drawn attention to its use as a piezoelectric transducer material [5,7]. Due to these promising piezoelectric properties, modified $PbTiO_3$ ceramics have been investigated by several authors. First, Ueda et. al. attempted to modify $PbTiO_3$ by adding MnO_2 and La_2O_3 and found a large anisotropy in coupling factor, with K_t=0.43 and K_p=0.096. [5] Takeuchi et. al. reported that $PbTiO_3$ ceramics modified with additives of Nd_2O_3, MnO_2 and In_2O_3 have zero temperature coefficients of surface acoustic wave delay time over a wide temperature range.[8] On the other hand, the phase transition in alkaline earth metal, Ba, Sr, Ca modified $PbTiO_3$ have been studied in 1951 by Shirane et. al. [3], however they could not obtain piezoelectric properties because of the difficulty in poling as a result of the poor insulating resistance. Yamashita et. al. attempted to modify $PbTiO_3$ by following Shirane et. al. result and adding Co and W. The composition $(Pb_{1-x}, Me_x)(Co_{1/2}W_{1/2})_{0.04}T_{0.96})O_3$ Me=CA, Sr and Ba and the largest anisotropy of coupling factor was found n the Ca modified $PbTiO_3$ ceramics poled under 50 Kv at 200°C, with K_t=0.53 and K_p=0.

In this study, Ca, Sr. and Ba modified $PbTiO_3$, $(Pb_{1-x}, Me_x)TiO_3$ Me=Ca, Sr and Ba were prepared by normal sintering processing. The lattice constant, crystal tetragonality and domain structures were examined by x-ray diffractmetry and transmission electron microscopy.

Experimental Procedure

All samples were weighed according to the formula, $(Pb_{1-x}Me_x)_ATi_BO_3$ + 1 mol%MnO (Me=Ca, Sr and Ba, X=0 to 0.4531, A/B=0.99). Starting raw

materials were chemically pure PbO(99.5%), TiO_2(99.7%), $CaCO_3$(99.8%) $SrCO_3$(99.6%), $BaCO_3$(99.7%) and MnO(99.3%). Mixed powders (x=0.125 to 0.4375 and x=0 and 0.0625) were calcined in an alumina crucible at 850°C and 800°C, respectively for 2 hours in air. After remilling using a polyethlene container and alumina balls for 5 hours and drying, calcined powders were pressed into cylinders(1 mm thick by 25 mm in diameter) under a uniaxial pressure of 1 ton/cm^2. The sintering temperatures varied according to composition as follows: for the Ca modified $PbTiO_3$, 1100°C to 1150°C for 2 hours. In the case of Sr and Ba modified $PbTiO_3$, these were 1200° C to 1250° C for 2 hours. With increasing values of x, the sintering temperature generally decreased.

Lattice constants were measured with an x-ray diffractometer using finely ground powders after sintering and scattering angles above 2θ=90 deg. Measured peaks were confirmed in the single phase field using the Hull-Davey chart and the extropolated values to $\cos^2\theta$=0 were used to obtain the lattice constant. Bulk density was measured by the water immersion method. Electron transparent samples were prepared by ion-milling and were examined at 100 kV in the Philips Em 301 and Em 400 microscopes using bright field and dark field imaging, diffraction and x-ray energy dispersive methods for elemental analysis.

Results and Discussion

The x-ray analysis indicated that except for the 45.31 mol%Ca modified $PbTiO_3$ all specimens were of the tetragonal perovskite structure. Figure 1 shows the variation of lattice parameters (a,c-lattice constant) in Ca, Sr and Ba modified $PbTiO_3$ as a function of modified content, x. With increasing

values of x, the c-axis of Ba, Sr modified $PbTiO_3$ decreased monotonically because $PbTiO_3$, $SrTiO_3$ and $BaTiO_3$ are all tetragonal at RT and easily combine into a solid solution. On the other hand, the c-axis of Ca modified $PbTiO_3$ sharply decreased when $x>0.375$, and with more than 45.31 mol% $CaTiO_3$, these ceramics exhibited a cubic crystal structure, in agreement with previous reports. [6] The a axis values depended on the type of modifying ions. With increasing x, the a parameter of Ba, Sr, and Ca modified $PbTiO_3$ increased, was constant, and decreased, respectively. These variations are simply explained in terms of the ionic radii of the added elements, e.g,, Ba(1.43Å), Sr(1.21Å), and Ca(1.03Å) which replace Pb ions (1.24Å). Figure 2 shows the variation in crystal tetragonality (i.e. c/a ratios) in Ca, Sr, and Ba modified $PbTiO_3$, as function of x. The c/a ratio of Sr and Ba modified $PbTiO_3$ decreased monotonically as did the variation of the c-axis. On the other hand, the c/a ratio of Ca modified $PbTiO_3$ shows the same change as that of Ba modified $PbTiO_3$ in a range of $x<0.375$, when the crystal anisotropy was large. However when $x>0.375$, the c/a ration sharply decreased, because of the phase transformation from tetragonal to cubic. In the cubic phase titanium ions occupy the body centered 1/2 1/2 1/2 position but may be displaced due to the presence of other ions. Figure 3 shows the volume changes of Ba, Ca and Sr modified $PbTiO_3$ as a function of x. In general, the remanent polarization of perovskite structure $(ABO)_3$ is proportional to the displacement of the B ion. As described in Figure 1, the a-axis was constant and the volume decreased in the case of Sr ion (same ionic radius as that of Pb ion), therefore it may be assumed that the Ti ion suffers minimum body centered cubic displacement and the

remanent polarization was decreased. On the other hand, in the case of Ca modified $PbTiO_3$ it may be predicted that the displacement of Ti from the 1/2 1/2 1/2 site would be larger, because of the decrease in both a-parameter and volume. Figure 4 shows plots of the theoretical and experimental density as a function of modifier content, x. The theoretical density was calculated from the lattice parameters obtained from the x-ray analysis, and all data are summarized in Table 1. As is shown, the porosity of Sr and Ca modified $PbTiO_3$ is less than 5% and 1.4% respectively, thus high density sintered bodies were prepared in this research.

Microstructures

Figure 5 shows typical domain structures of Ca and Sr modified $PbTiO_3$. These structures are observed in many non-cubic systems , e.g., ordered alloys, martensitically transformed materials and are present to minimize strains and shape deformation [9]. As can be depicted in Fig. 5A, many small domains can be observed in one grain. The angular relationship among these domains is 90^o and the direction of the domain boundary is ‹100›, therefore these domains were concluded to be 90^o domains. Such 90^o "a-c" domains can be clearly seen in Sr modified $PbTiO_3$ as shown in Fig. 5b. The "a" domain bordered on "c" with the angle of 45^o, therefore delta fringes can be observed across domain boundaries[10]. The grain sizes and domain widths are summarized in Table II. The results show that both grain size and domain size are almost constant in spite of changing the values of x. The ratio of grain size and domain width are the same for Ba and Ca modified $PbTiO_3$, but that of Sr modified $PbTiO_3$ is considerably (about 1/20) smaller than that of Ca and Ba modified $PbTiO_3$. In general, these domains form immediately in the ferroelectric region

corresponding to the cubic→tetragonal transformation at the Curie point. The domain configuration adopted is that corrresponding to minimum lattice distortion (c/a ratio). Consequently, it was concluded that the strain energy due to lattice distortion of the Sr modified $PbTiO_3$ is smaller than that of Ba and Ca modified $PbTiO_3$.

Figure 6 shows strain contrast corresponding to abutting domains along the grain boundary. This result shows that more lattice distortion exists than that released by construction of the intragranular domain configurations in 12.5 mol% Ca modified $PbTiO_3$. Figure 7 indicates where nucleation of domains in Ca and Ba modified $PBTiO_3$ can occur. These 90^o "a-c" wedged-shaped domains seem to nucleate from the grain boundary (Fig. 7a) and domain boundary (Fig. 7b). In other words 90^o "a-c" domains were frequently nucleated at strained regions, domain and grain boundaries and at cracks in the samples. Transparent, strain free grains as shown in Fig. 8 can be sometimes observed in Ca modified $PbTiO_3$. X-ray (EDX) analysis indicates these grains to contain a large amount of Ti and very small amounts of Mn, and Pb. This localized TiO_2 particle is present due to the excess TiO_2 added to provide liquid phase sintering. Electron diffraction analyses later revealed the ordered cubic structure in 45.31 mol% Ca modified $PbTiO_3$. Diffraction patterns taken in [110] and [100] zone axes are shown in Fig. 9 a and b respectively. The lattice parameter calculated from the intense spots coincided with that obtained from x-ray analysis. This diffraction pattern was cubic fcc and the extra weak spots occur between those which describe the basic unit cell. As a result, all diffraction spots were indexed as shown in Fig. 9a. The calculated lattice parameters were twice that of the standard lattice

parameters in $PbTiO_3$. On the other hand, the ordering is weak as evidenced from the low superlattice intensities.

Figure 10 shows the bright field (BF) and dark field (DF) images of ordered structure in Fig. 9. The DF image was taken using the [111] superlattice reflection. The contrast is reversed and there appear to be antiphase boundaries (dark, wavy regions). Figure 11 shows the diffraction patterns of 43.75 mol% Ca modified $PbTiO_3$ with small tetragonality (lower x values) As can be seen, superlattice reflections as in Fig. 9 could not be observed. The same result has been obtained in transparent PLZT, (La modified PZT) after the tetragonal to cubic transformation [11].

Figure 12 are micrographs in which another phase has been detected in the $(Pb_{0.76}Ca)(Co_{1/2}W_{1/2})_{0.04}Ti_{0.96})O_3$ + 1 mol%MnO sample [7]. From the x-ray EDS spectrum (Fig. 13), the composition of plate like crystals (Fig. 2a) were calculated to be $Pb_{0.79}TiO_3$ + 0.047CoO + 0.019 MnO. Although Ca was not detected in this crystal, Co and Mn ions were present in much higher concentrations as compared to that of the matrix. From these results, it was concluded that this phase was $PbTiO_3$ containing Co and Mn. As shown previously [7] Ca modified $PbTiO_3$ has a large anisotropy in piezoelectric property, as that in pure $PbTiO_3$. Thus, it can assumed that the presence of the new phase contributes to the large anisotropy in Ca modified $PbTiO_3$ in spite of its small volume fraction (about 0.02 vol %). On the other hand, the compositions of the phase in Fig. 12b was Ca/Ti/Mn/Co/Zr/Pb=67.6/2.2/2.4/3.5/22.8/1.5 at.%. The Zr was due to contamination during powder processing. It can be assumed that this

phase is Ca_3ZrO_5 (from electrical neutrality condition) with a small amount of Ti, Mn, Co, and Pb. Its volume fraction was about 0.12 vol%. Further investigations of these inclusions are required because unique identification of Ca_3ZrO_3 is not yet confirmed.

Summary

The results obtained in this study of modified $PbTiO_3$ are summarized as follows:

1. The c/a ratio changed linearly as a function of the amount of modifier content, x, and its change with Ca and Ba added $PbTiO_3$ was almost the same when the value of x was below 35 mol%.
2. From the c/a ratio and volume change, it could be expected that the remanent polarization in Ca and Ba modified $PbTiO_3$ will not be much decreased in spite of the large amount of modifying ions present.
3. Lattice strains develop at grain boundaries due to impingement of domains in Ca modified $PbTiO_3$.
4. Superlattice structures having twice the lattice constants compared to standard $PbTiO_3$ were observed in cubic Ca modified $PbTiO_3$.
5. In the $(Pb_{0.76}Ca_{0.24})(Co_{1/2}W_{1/2})_{0.04}Ti_{0.96})O_3$ + 1 mol%MnO ceramics two unique inclusions were found and these compositions were determined by x-ray microanalysis.

Acknowledgement

This work was supported by the Director, Office of Energy Research, Office of Basic Energy Sciences, Materials Sciences, Division of the U. S. Department of Energy under contract No. DE-AC03 -76SF00098.

References

1. B. Jaffee, R. Cook and H. Jaffee, Piezoelectric Ceramic, Adacemic Press New York, 351 (1971).

2. T. Y. Tein and W. G. Carlson, J. Am. Ceram. Soc., 45 (12) 567 (1962).

3. G. Shirane and S. Hoshino, J. Phy. Soc. Japan, 6 (4) 274 (1951).

4. K. Okazaki and K. Takashasi, Memo. Natl. Defense Acad. 5 (2) 183 (1967).

5. I. Ueda and S. Ikegami, Jpn.J. Appl. Phys., 7 (3) 236 (1968).

6. E. Sawaguchi and M. L. Carters, J. Amer. Ceram. Soc.,42 (4) 157 (1959).

7. Y. Yamashita, K. Yokoyama, H. Honda and T. Takahashi, Jpn. J. Appl. Phy., 20, Suppl. 2-4, 183 (1981).

8. Y. Ito, H. Takeuchi, K. Nagatsuma, S. Jyomura and S. Ashida, J. Appl. Phys. 52, 3223 (1981).

9. The theory is treated in detail in A. Khachaturyan, "Theory of Structural Phase Transformations in Solids", J. Wiley (N.Y.) 1963.

10. R. Vikagrana and G. Thomas, Phys. Stat. Sol., 9, 499 (1965).

11. T. Yamamoto, unpublished research.

Figure Captions

Fig. 1. Lattice parameters (c, a-axis) of Ca, Sr, and Ba modified $PbTiO_3$ as a function of modifier content.

Fig. 2. Crystal tetragonality (c/a) of Ca, Sr, and Ba modified $PbTiO_3$ as a function of modifier amount.

Fig. 3. Volume changes vs. modifier amount using the volume of pure $PbTiO_3$ as reference point.

Fig. 4. Theoretical and experimental density of Ca, Sr, Ba modified $PbTiO_3$ as a function of modifier amount.

Fig. 5. Domain structures of Ca and Sr modified $PbTiO_3$ $PC_{0.125}$=12.5 mol% Ca modified $PbTiO_3$.

Fig. 6. Strain contrast contours indicating internal stress of grain boundary in Ca modified $PbTiO_3$.

Fig. 7. Electron micrograph indicating nucleation of domains in Ca, Ba modified $PbTiO_3$.

Fig. 8. Inclusion of TiO_2 detected in CA modified $PbTiO_3$, left, electron micrograph, right, EDX spectrum from inclusion.

Fig. 9. Electron diffraction patterns showing ordered structure of cubic modified $PbTiO_3$.

Fig. 10. BF and DF electron microscope images in the ordered structure.

Fig. 11. Diffraction pattern taken by ZA=[110 and [100] in the Ca modified $PbTiO_3$ with a small tetragonality.

Fig. 12. Other phases in $(Pb_{0.76}Ca_{0.24})$ $(Co_{1/2}W_{1/2})Ti_{0.96})O_3$ + 1 mol%MnO.

Fig. 13. EDX spectrums of other phases and matrix.

$(Pb_{1-x}M)TiO_3$: M= Ca, Sr, Ba X=0~0.453

PM_x	lattice const. a axis (Å)	lattice const. c axis (Å)	crystal tet. (c/a)	volume change $(V - V_0/V_0) \times 100$	theoretical density (g/cm^3)	experimental density (g/cm^3)	porosity (%)
PC_0	3.9045+0.0022	4.1521+0.0038	1.063		7.896		
$PC_{0.0625}$	3.8907+0.0013	4.1148+0.0924	1.058	-1.6862	7.744		
$PS_{0.0625}$	3.9113+0.0054	4.1052+0.0241	1.050	-0.7835	7.762	7.50	3.38
$PB_{0.0625}$	3.9131+0.0016	4.1382+0.0138	1.058	+0.1042	7.772	7.31	5.94
$PC_{0.1250}$	3.8934+0.0042	4.0800+0.0103	1.048	-2.2942	7.526	7.48	0.61
$PS_{0.1250}$	3.9151+0.0034	4.0788+0.0574	1.042	-1.2114	7.600	7.38	2.89
$PB_{0.1250}$	3.9177+0.0040	4.1281+0.0064	1.054	+0.0981	7.661	7.49	2.23
$PC_{0.1825}$	3.8915+0.0022	4.0743+0.0194	1.047	-2.5313	7.227	7.19	0.51
$PS_{0.1825}$	3.9160+0.0007	4.0560+0.0453	1.036	-1.7367	7.477	7.19	3.84
$PB_{0.1825}$	3.9280+0.0080	4.1065+0.0507	1.045	-0.1756	7.573	7.26	4.13
$PC_{0.2500}$	3.8934+0.0076	4.0440+0.0085	1.039	-3.1507	7.032	6.94	1.30
$PS_{0.2500}$	3.9050+0.0027	4.0150+0.0036	1.028	-3.4047	7.439	7.09	4.69
$PB_{0.2500}$	3.9421+0.0068	4.0864+0.0045	1.037	+0.3231	7.418	7.35	0.92
$PC_{0.3125}$	3.8914+0.0057	4.0234+0.0211	1.034	-3.5171	6.847	6.76	1.24
$PS_{0.3125}$	3.9085+0.0040	3.9968+0.0185	1.023	-3.5437	7.180	6.86	4.46
$PB_{0.3125}$	3.9443+0.0040	4.0778+0.0211	1.034	+0.2243	7.312	7.12	2.63
$PC_{0.3750}$	3.8913+0.0026	3.9860+0.0080	1.024	-4.6526	6.574	6.55	0.37
$PS_{0.3750}$	3.8978+0.0080	3.9608+0.0468	1.016	-4.9338	7.081	6.79	4.11
$PB_{0.3750}$	3.9466+0.0046	4.0599+0.0263	1.029	-0.0982	7.222	7.08	1.97
$PC_{0.4375}$	3.8968+0.0042	3.9140+0.0053	1.004	-6.1088	6.387	6.32	1.05
$PS_{0.4375}$	3.8991+0.0040	3.9399+0.0035	1.010	-5.3743	6.909	6.63	4.04
$PB_{0.4375}$	3.9543+0.0064	4.0518+0.0051	1.025	+0.0872	7.027	6.69	4.80
$PC_{0.453}$	3.8980+0.0063	3.8980+0.0063	1.000	-6.4317	6.337	6.25	1.37

volume change : V_0= $PbTiO_3$ volume (PC_0) , crystal tet.= crystal tetragonality

XBL 857-3150

Table I

SAMPLE	GRAIN SIZE (μM)	DOMAIN WIDTH (μM)
$PC_{0.0625}$	X	X
$PB_{0.0625}$	0.7	0.043
$PS_{0.0625}$	64.9	0.13
$PC_{0.125}$	1.43	0.09
$PB_{0.125}$	0.93	0.06
$PS_{0.125}$	35.7	0.36
$PC_{0.185}$	1.41	0.09
$PB_{0.185}$	0.90	0.06
$PS_{0.185}$	62.5	0.20
$PC_{0.25}$	1.40	0.09
$PB_{0.25}$	1.14	0.06
$PS_{0.25}$	32.9	0.17
$PC_{0.3125}$	1.35	0.09
$PB_{0.3125}$	1.21	0.06
$PS_{0.3125}$	68.4	0.19
$PC_{0.375}$	1.03	0.10
$PB_{0.375}$	1.30	0.06
$PS_{0.375}$	50.5	0.18
$PC_{0.4375}$	1.25	*
$PB_{0.4375}$	1.25	0.09
$PS_{0.4375}$	1.25	0.14
$PC_{0.4531}$	1.36	*

X : BROKEN, NOT SINTERED

* : NO DOMAIN, CUBIC

Table II

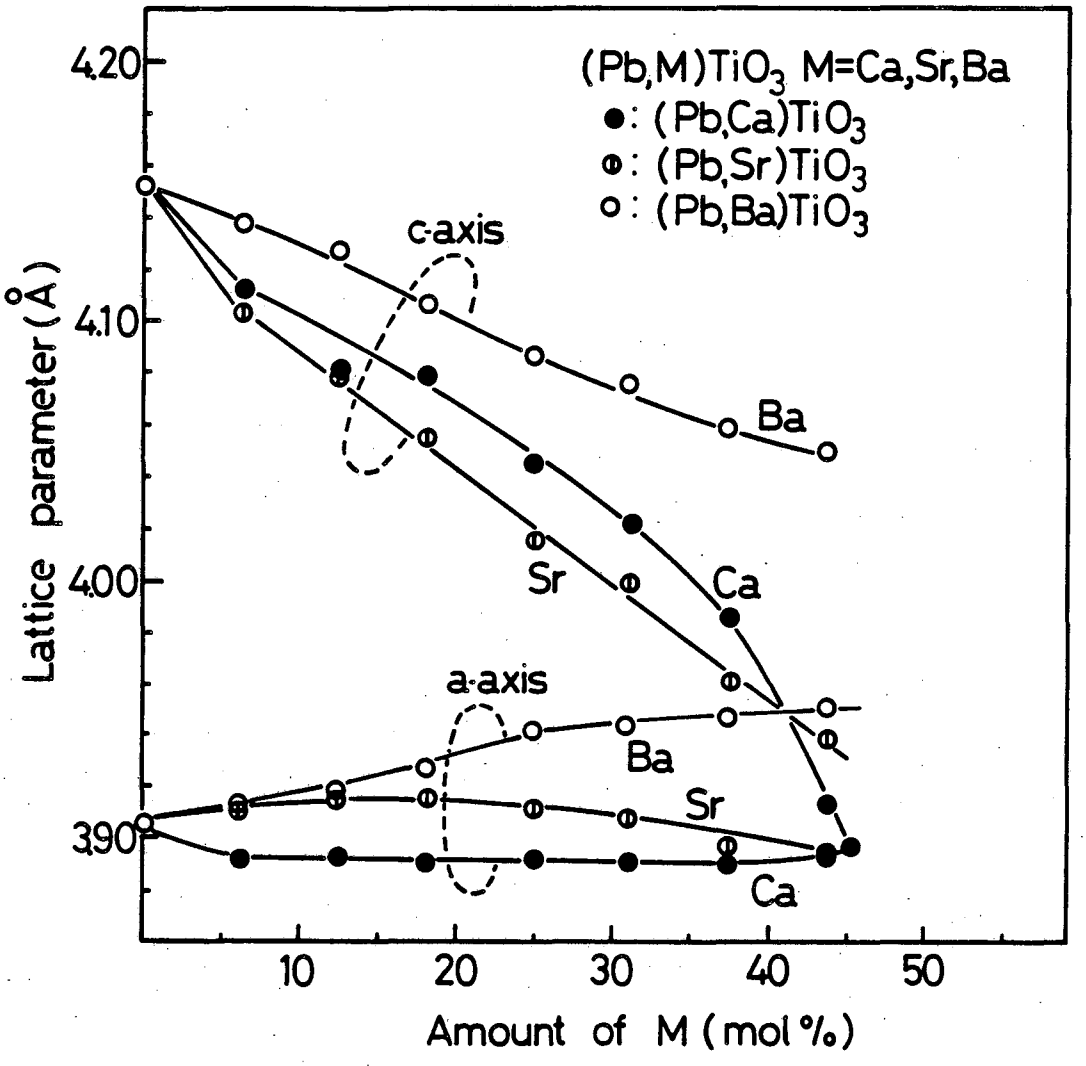

XBL 857-3163

Fig. 1

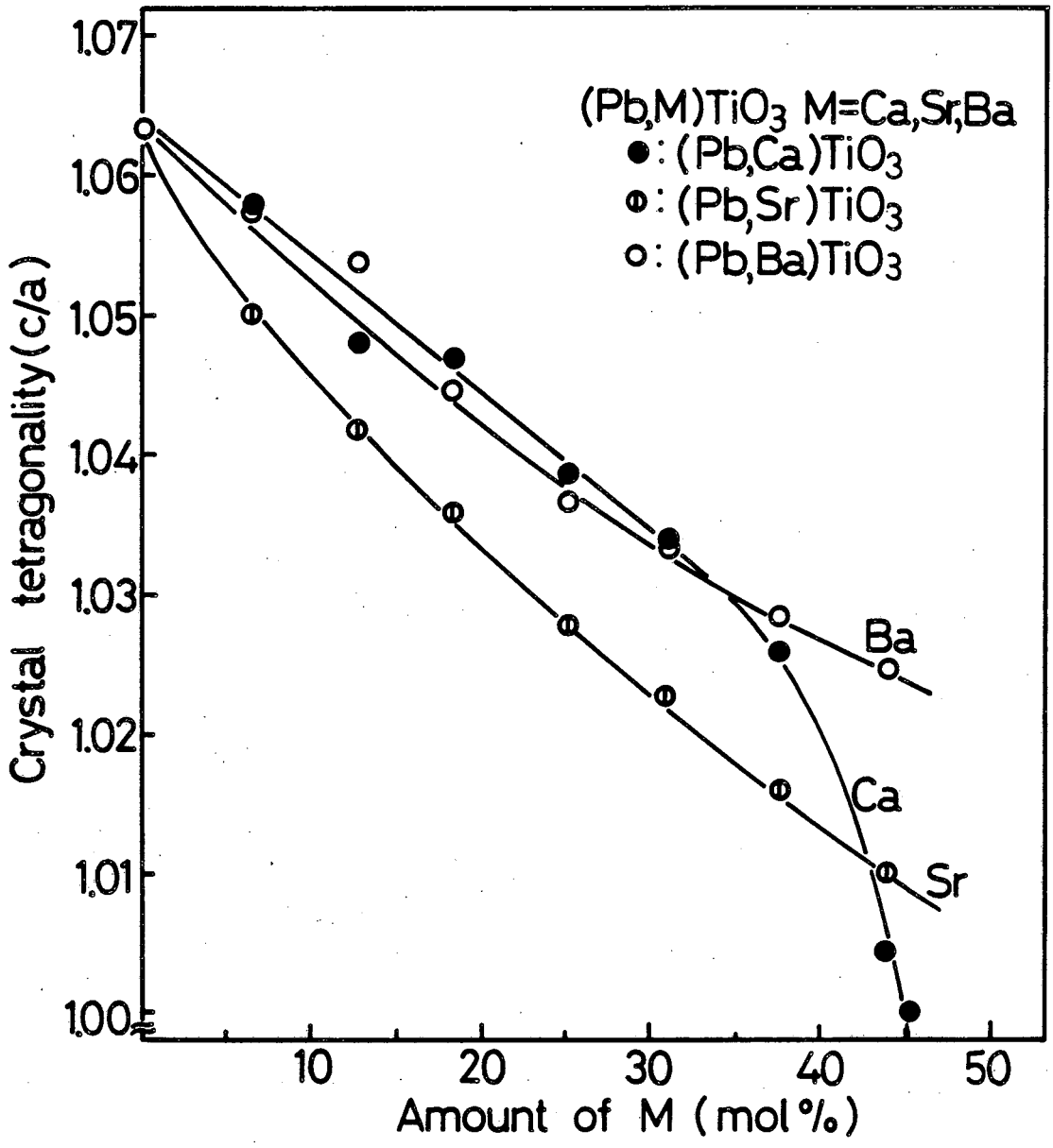

XBL 857-3164

Fig. 2

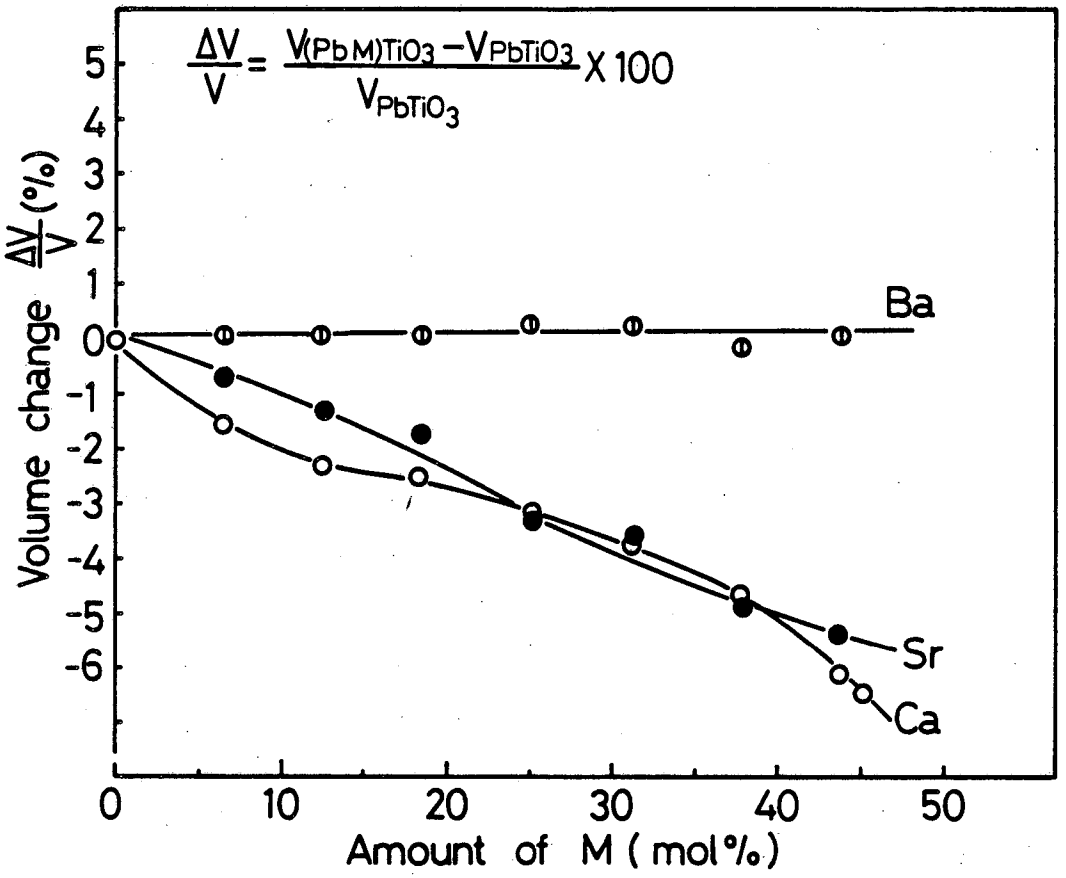

XBL 857-3161

Fig. 3

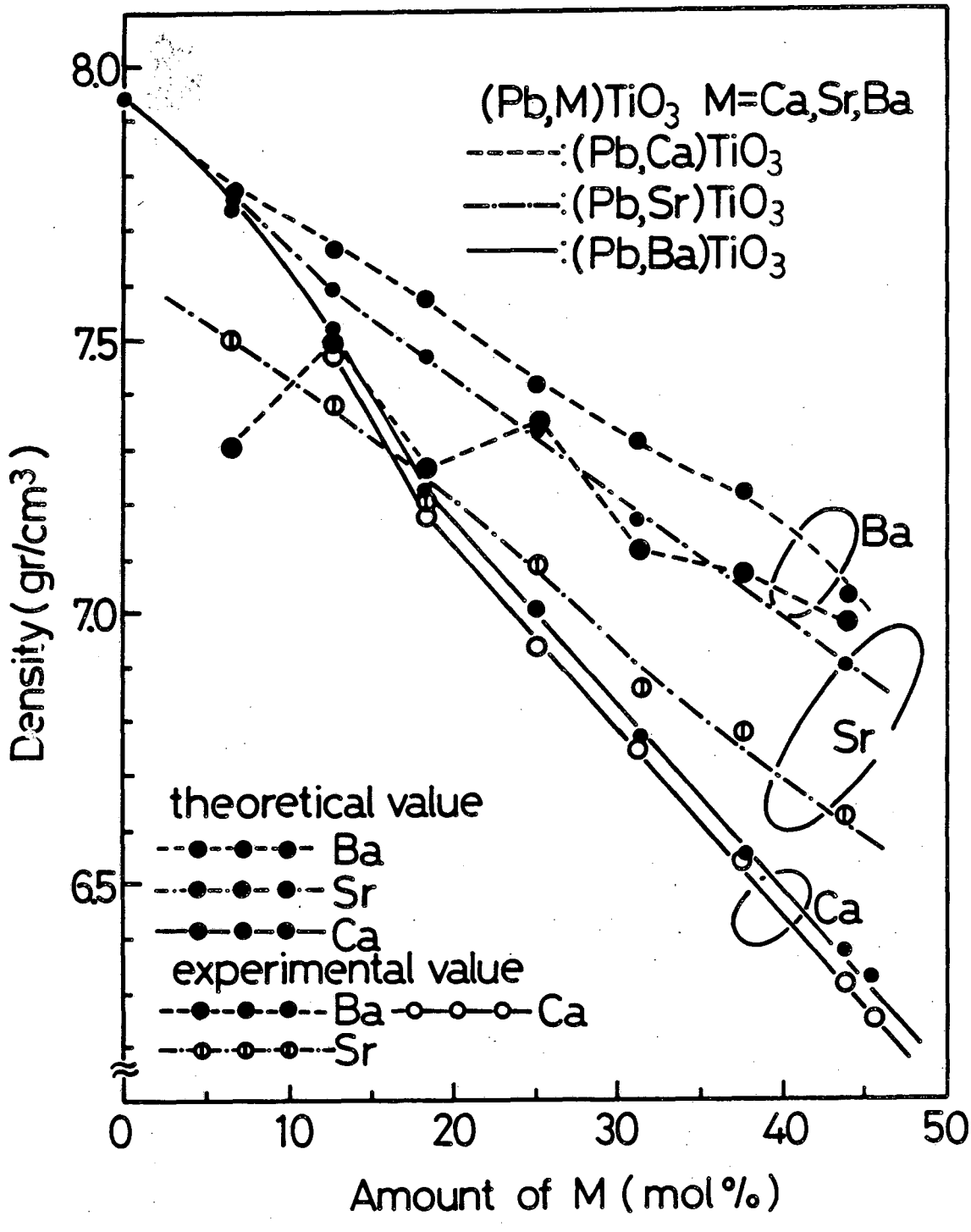

XBL 857-3162

Fig. 4

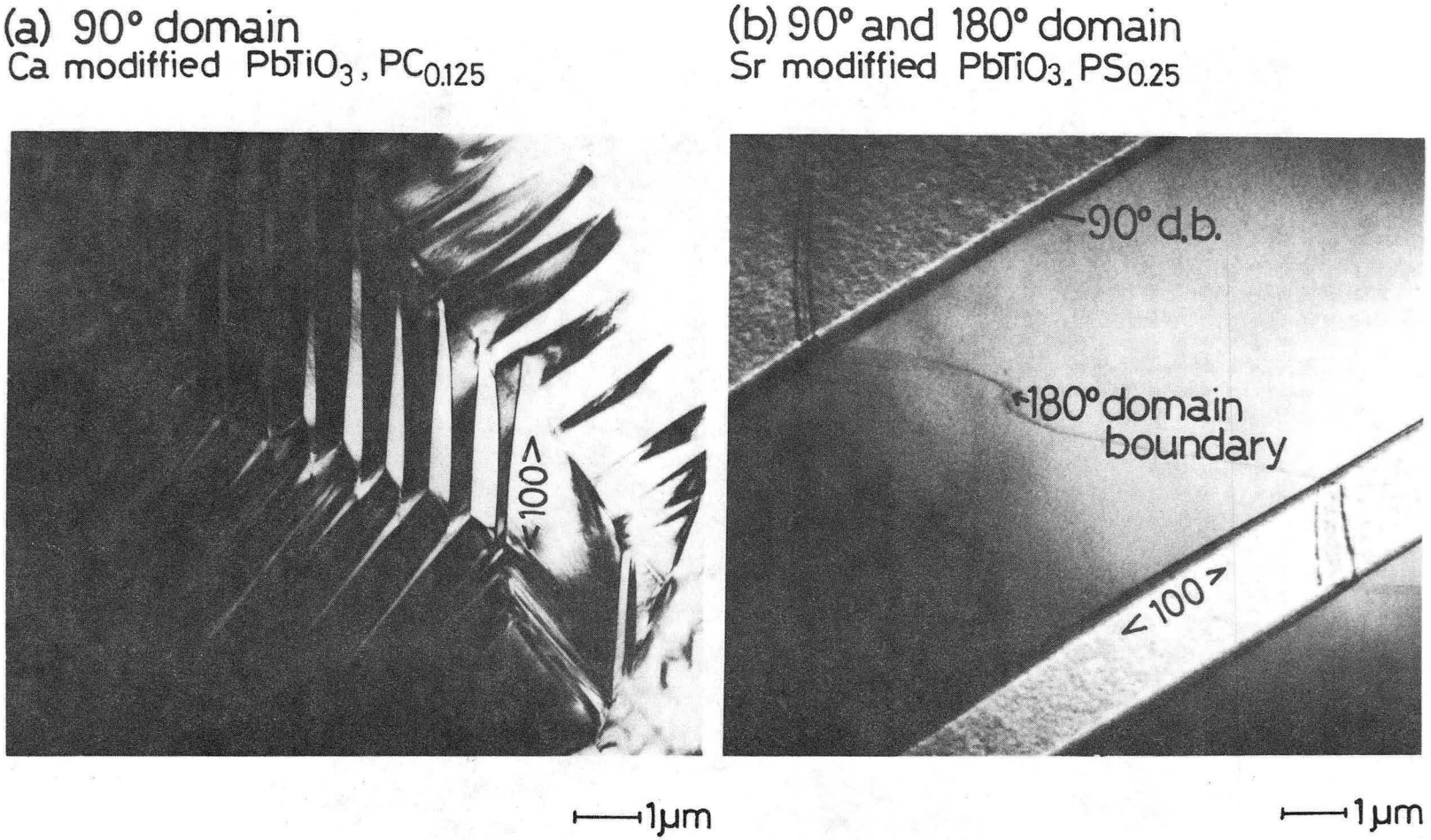

XBB 859-7290

Fig. 5

Stress distribution
Ca modiffied $PbTiO_3$, $PC_{0.125}$

XBB 859-7289

Fig. 6

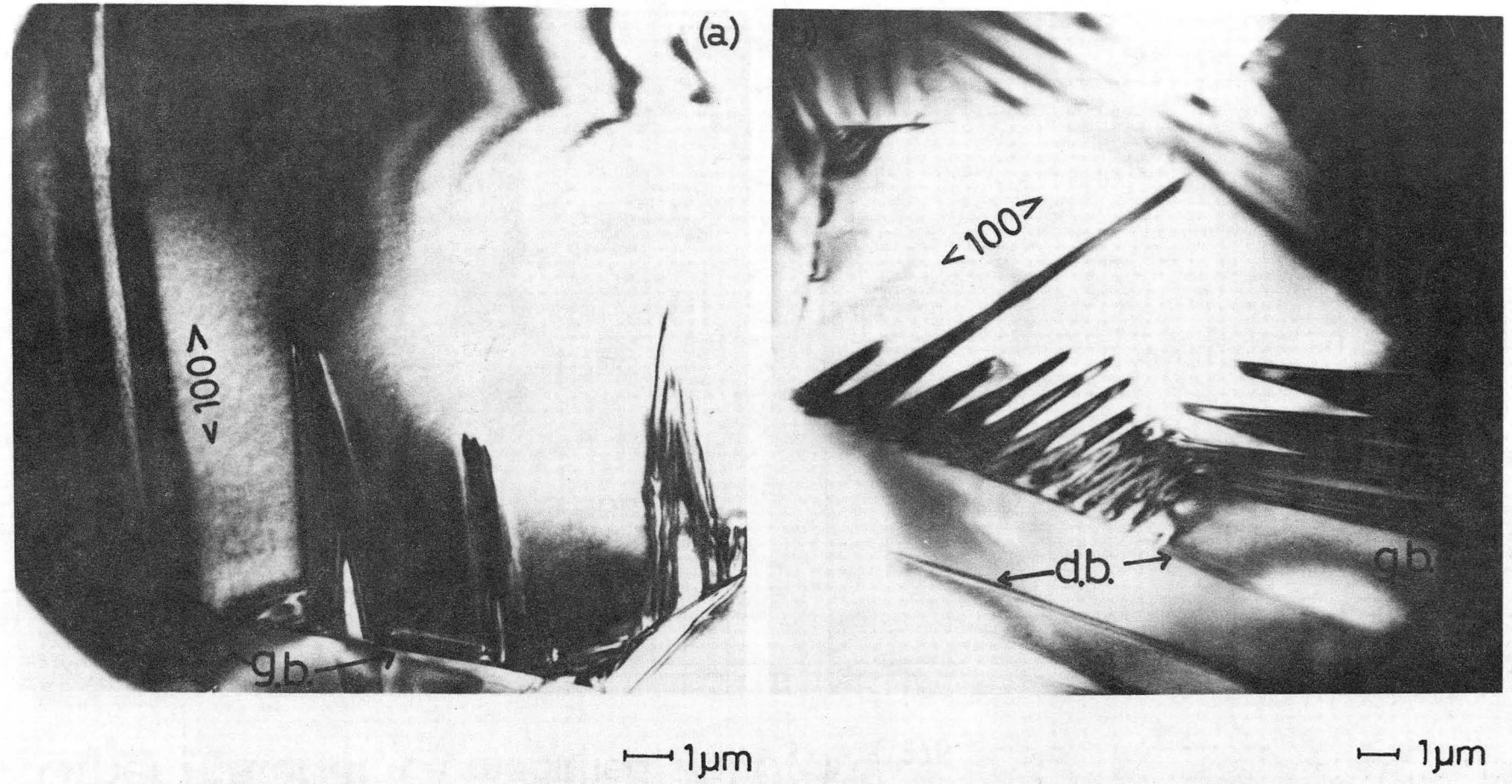

XBB 859-7291

Fig. 7

Other material, Ca modiffied $PbTiO_3$, $PC_{0.375}$

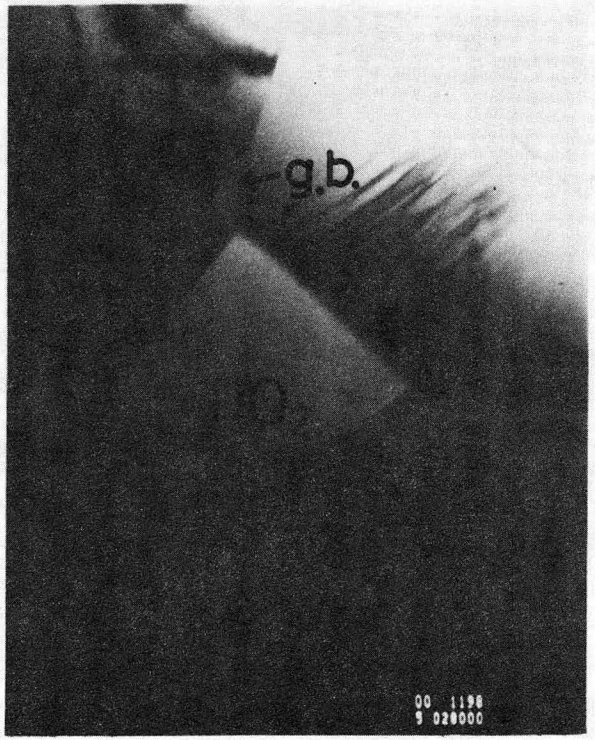

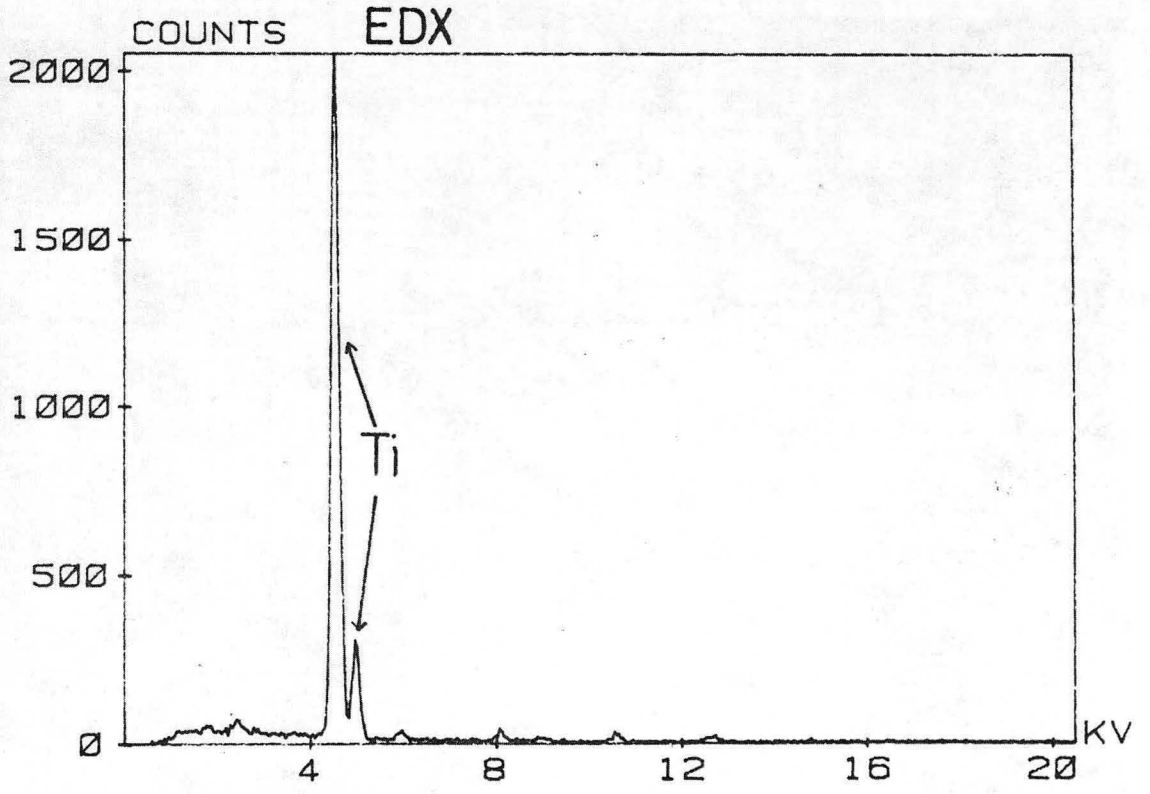

Fig. 8

XBB 859-7294

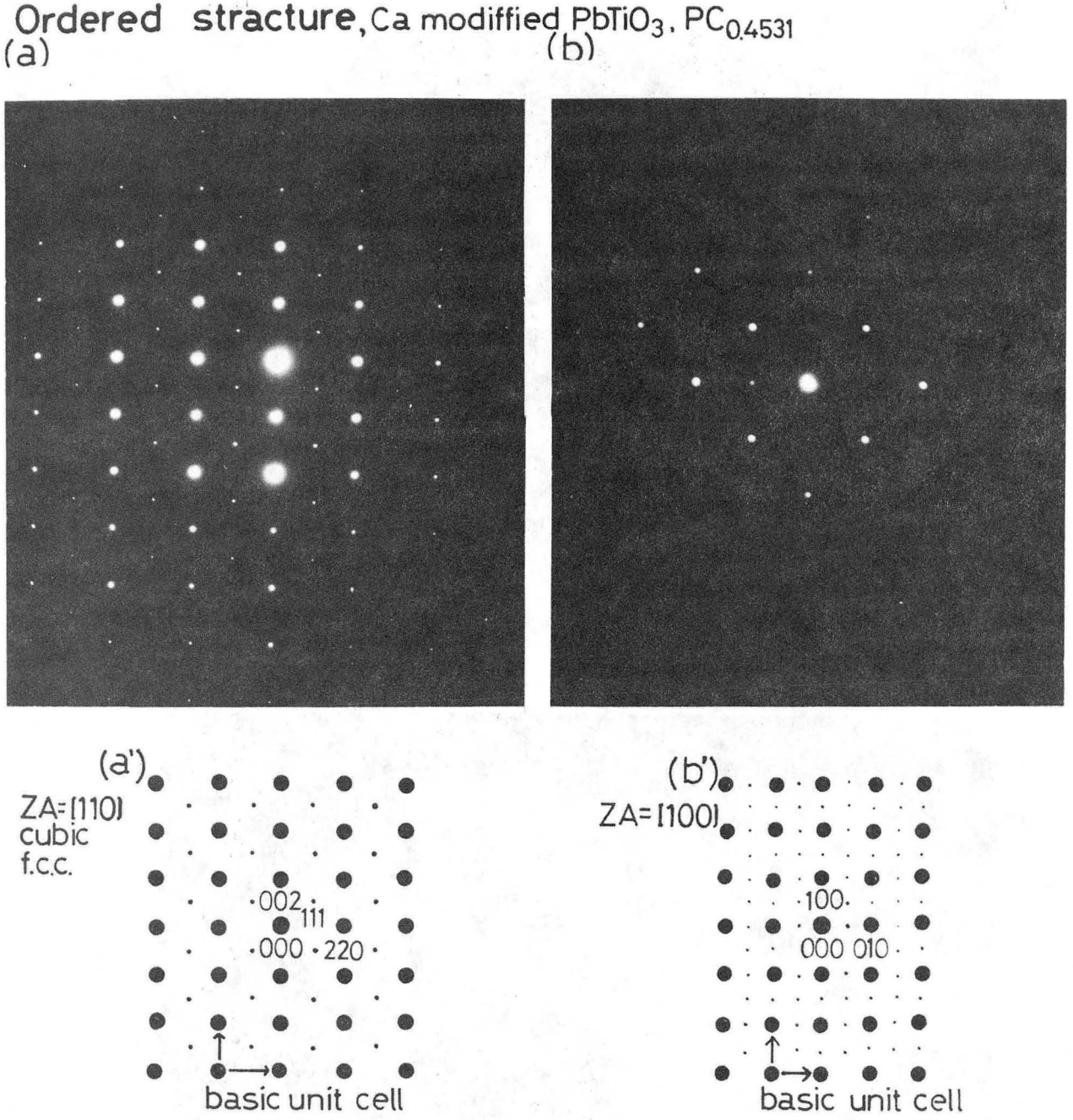

XBB 859-7292

Fig. 9

(a) BF

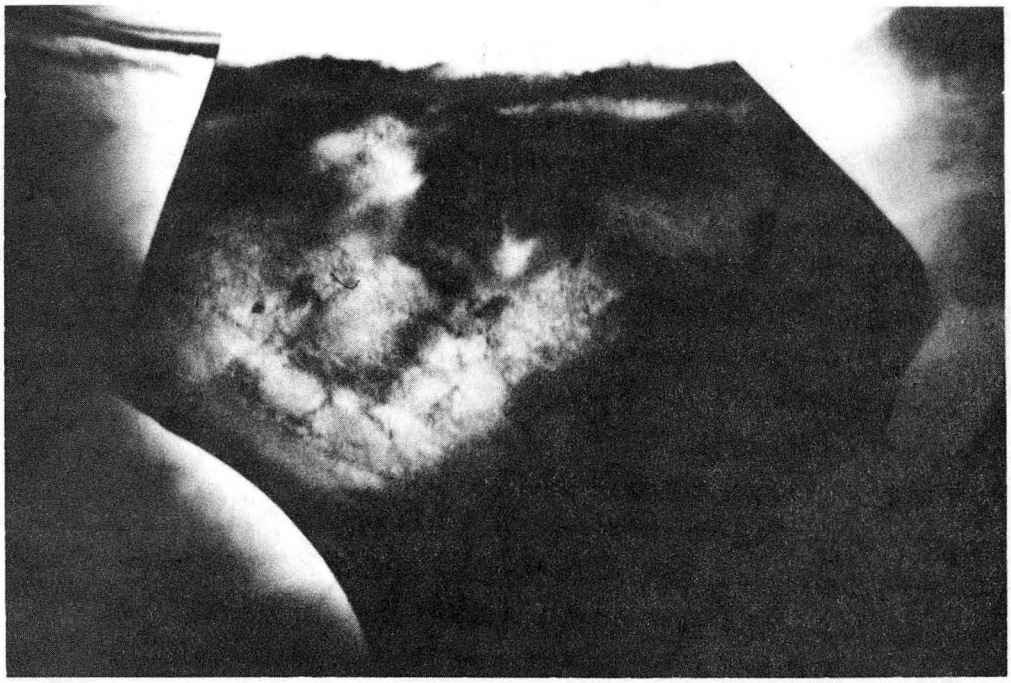

(b) DF

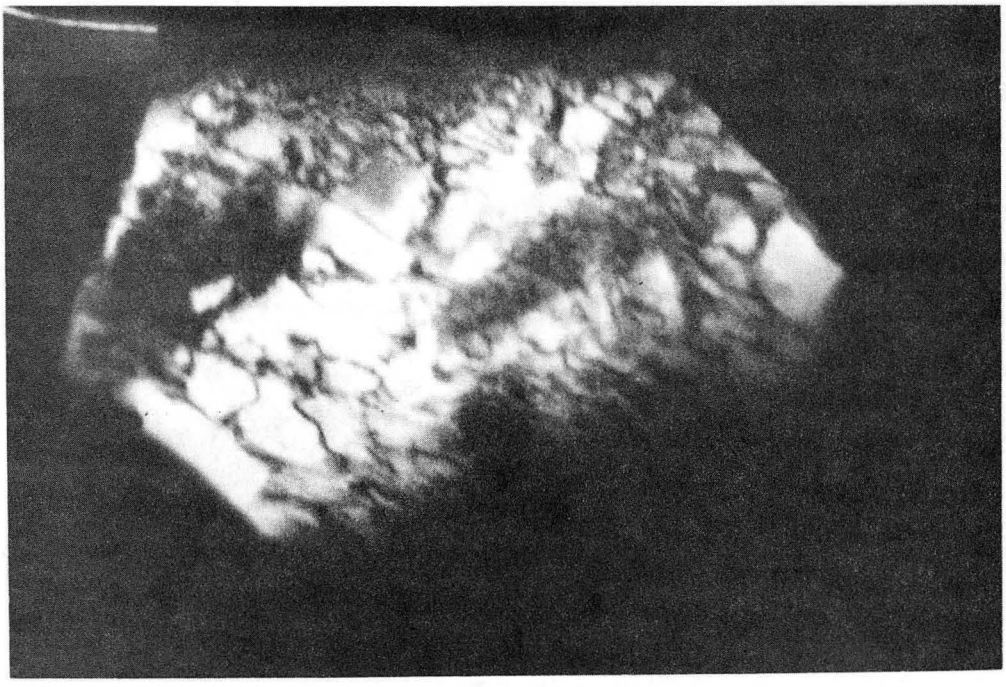

H 1μm

H 1μm

Fig. 10 XBB 859-7288

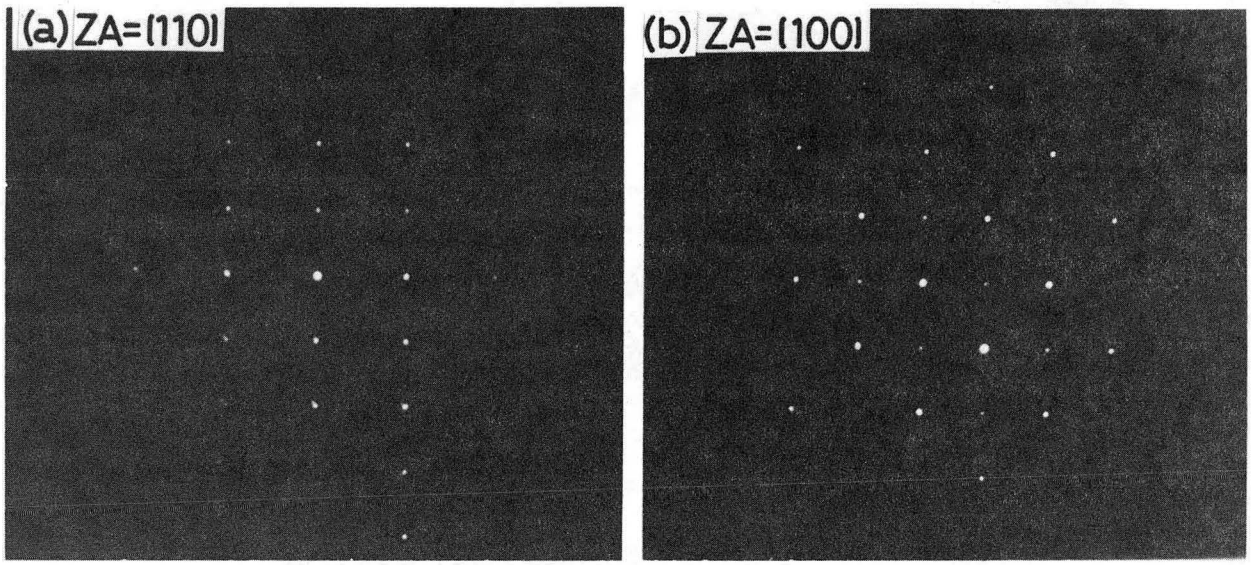

Fig. 11

XBB 859-7295

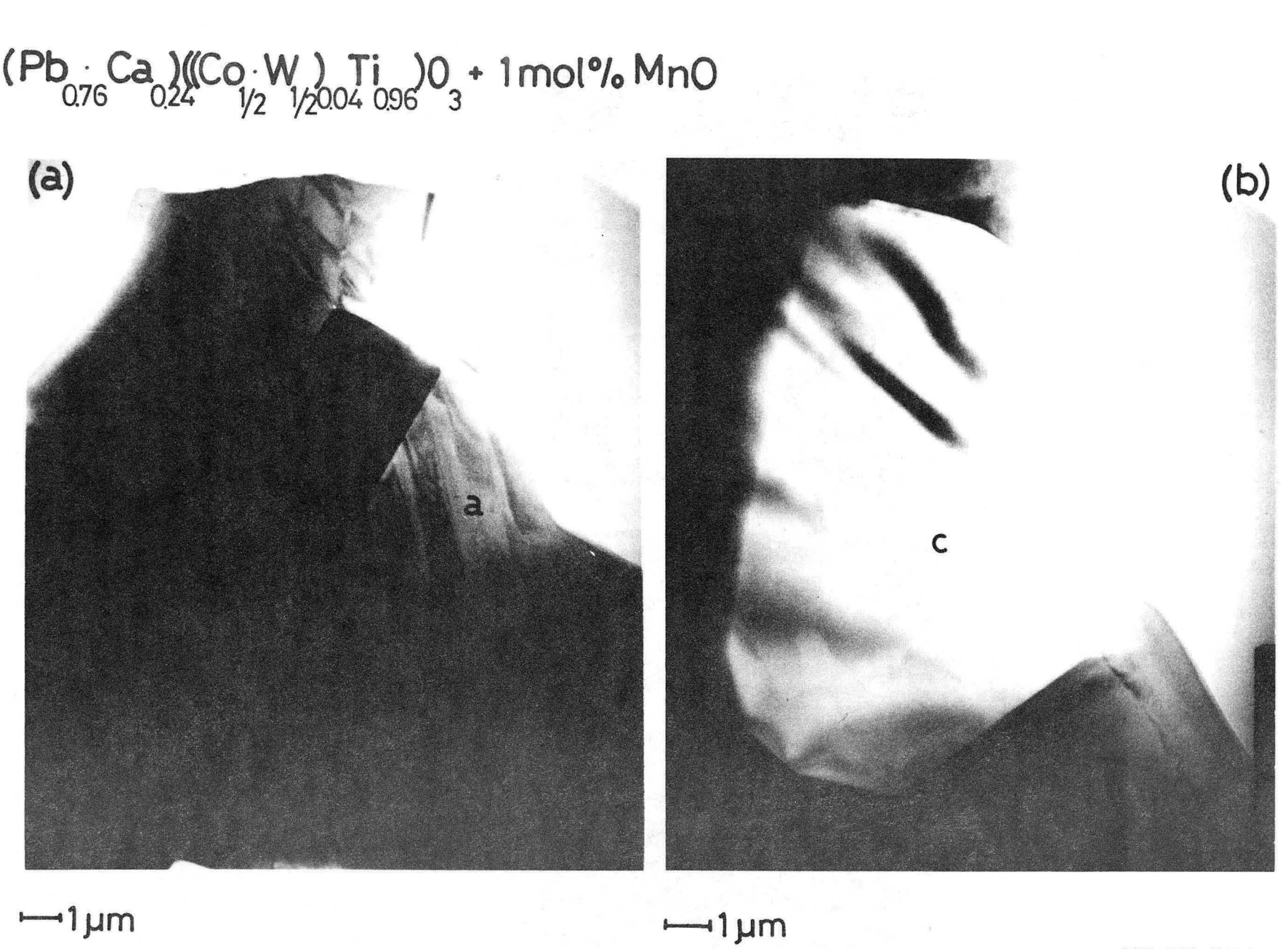

XBB 859-7293

Fig. 12

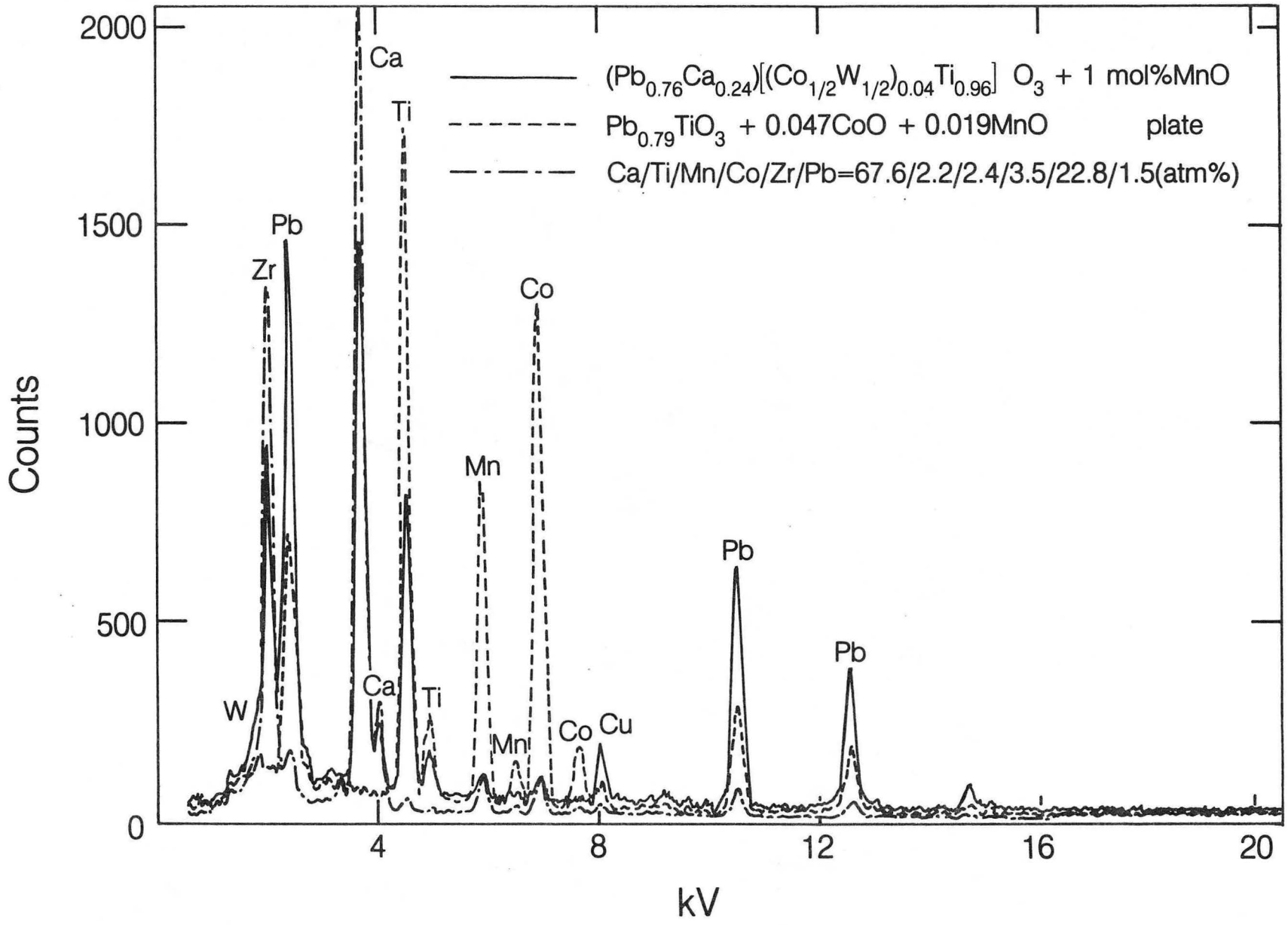

Fig. 13

XBL 862–10310

This report was done with support from the Department of Energy. Any conclusions or opinions expressed in this report represent solely those of the author(s) and not necessarily those of The Regents of the University of California, the Lawrence Berkeley Laboratory or the Department of Energy.

Reference to a company or product name does not imply approval or recommendation of the product by the University of California or the U.S. Department of Energy to the exclusion of others that may be suitable.

LAWRENCE BERKELEY LABORATORY
TECHNICAL INFORMATION DEPARTMENT
UNIVERSITY OF CALIFORNIA
BERKELEY, CALIFORNIA 94720